LETTER

# Optical emission spectrum of filamentary nanosecond surface dielectric barrier discharge

To cite this article: S A Shcherbanev *et al* 2017 *Plasma Sources Sci. Technol.* **26** 02LT01

View the article online for updates and enhancements.

## Related content

- A nanosecond surface dielectric barrier discharge in air at high pressures and different polarities of applied pulses: transition to filamentary mode
S A Stepanyan, A Yu Starikovskiy, N A Popov et al.
- Nanosecond surface dielectric barrier discharge in atmospheric pressure air: I. measurements and 2D modeling of morphology, propagation and hydrodynamic perturbations
Yifei Zhu, Sergey Shcherbanev, Brian Baron et al.
- Evolution of nanosecond surface dielectric barrier discharge for negative polarity of a voltage pulse
V R Soloviev, V M Krivtsov, S A Shcherbanev et al.

## Recent citations

- Analysis and Processing of Spark Channel Interferograms Obtained by Picosecond Laser Interferometry
A. I. Khirianova *et al*
- Fast fine-scale spark filamentation and its effect on the spark resistance
E V Parkevich *et al*
- Filamentary nanosecond surface dielectric barrier discharge. Experimental comparison of the streamer-to-filament transition for positive and negative polarities
Ch Ding *et al*

IOP ebooks™

Bringing you innovative digital publishing with leading voices to create your essential collection of books in STEM research.

Start exploring the collection - download the first chapter of every title for free.

This content was downloaded from IP address 93.180.48.67 on 24/10/2019 at 11:50

Letters

IOP Publishing

Plasma Sources Science and Technology

Plasma Sources Sci. Technol. **26** (2017) 02LT01 (7pp)

doi:10.1088/1361-6595/26/2/02LT01

Letter

# Optical emission spectrum of filamentary nanosecond surface dielectric barrier discharge

**S A Shcherbanev[1], A Yu Khomenko[2], S A Stepanyan[1], N A Popov[3] and S M Starikovskaia[1]**

[1] Laboratory of Plasma Physics (CNRS, Ecole Polytechnique, Sorbonne Universities, University of Pierre and Marie Curie-Paris 6, University Paris-Sud), Ecole Polytechnique, route de Saclay, 91128 Palaiseau, France

[2] Moscow Institute of Physics and Technology, Institutskii lane, 9, Dolgoprudny 141700, Russia

[3] Skobeltsyn Institute of Nuclear Physics, Moscow State University, Moscow, 119991, Leninsky gory, Russia

E-mail: sergey.shcherbanev@lpp.polytechnique.fr and svetlana.starikovskaya@lpp.polytechnique.fr

Received 16 August 2016, revised 14 November 2016
Accepted for publication 17 November 2016
Published 23 December 2016

**Abstract**

Streamer-to-filament transition is a general feature of high pressure high voltage (HV) nanosecond surface dielectric barrier discharges. The transition was studied experimentally using time- and space-resolved optical emission in UV and visible parts of spectra. The discharge was initiated by HV pulses 20 ns in duration and 2 ns rise time, positive or negative polarity, 20–60 kV in amplitude on the HV electrode. The experiments were carried out in a single-shot regime at initial pressures $P > 3$ bar and ambient initial temperature in air, $N_2$, $H_2$:$N_2$ and $O_2$:Ar mixtures. It was shown that the transition to filamentary mode is accompanied by the appearance of intense continuous radiation and broad atomic lines. Electron density calculated from line broadening is characterized by high absolute values and long decay in the afterglow. The possible reasons for the continuous spectra were analyzed.

Keywords: nanosecond SDBD, filaments, discharge at high pressure, emission spectroscopy

(Some figures may appear in colour only in the online journal)

## 1. Introduction

Nanosecond surface dielectric barrier discharges (nSDBD) are developed for flow control applications [1, 2], laser pumping [3], and plasma-assisted combustion [4–6]. It was found recently [7] that at a pressure and/or voltage increase, a single-shot nSDBD transforms into a filamentary form. Streamers start from the high voltage (HV) electrode, slow down and stop. At this instant, a few nanoseconds after the discharge initiation, a set of bright filaments starts from the HV electrode. The number of filaments is four to five times less than the initial number of streamers.

Streamer-to-filament transition is a general feature of nanosecond surface discharges at high pressures [8]: filamentation was observed for both polarities of voltage, different dielectrics, and in different gases. Critical pressure $P_c$ and voltage $V_c$ when the filamentation occurs are the functions of polarity and gas mixture. Filamentary discharges ignite combustible mixtures at initial gas pressures up to 15 bar [8, 9]; very specific regimes, when the mixture ignites simultaneously along multiple discharge channels, were observed at high pressures. The simultaneous uniform ignition along the filaments proves, although indirectly, that the specific deposited energy in the filaments is high. At the same time, the

 © 2016 IOP Publishing Ltd Printed in the UK

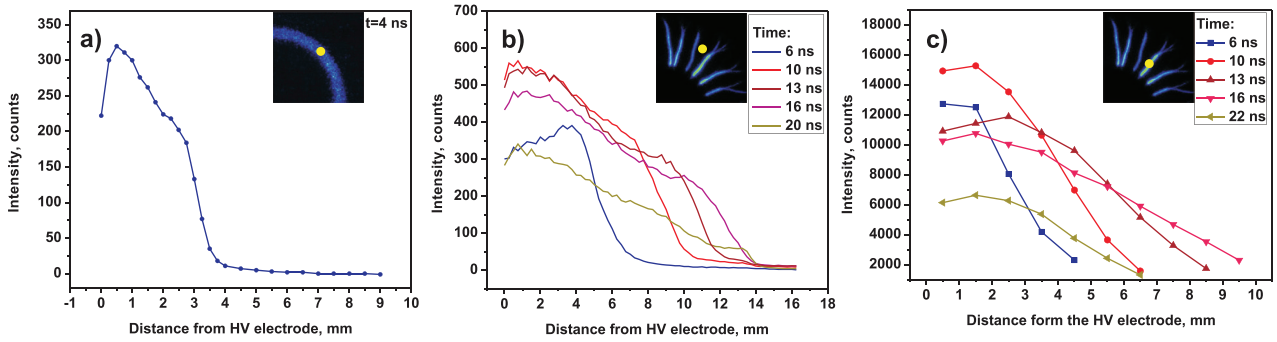


**Figure 1.** Relative intensity of $\lambda = 300$–$800$ nm emission in (a) streamer mode; (b) between the filaments; and (c) in the filaments versus distance from the edge of the HV electrode at different time instants. Synthetic air, $U = -47$ kV, $P = 3$ bar. ICCD images, gate 2 ns, are given as inserts.

information about the parameters of plasma in the filaments is practically absent. The aim of the present work is to study the behavior of the filamentary nSDBD using time- and space-resolved emission spectroscopy.

## 2. Experimental setup

Two electrode systems in a coaxial configuration are described elsewhere [7, 8]. A metal disk 20 mm in diameter served as a HV electrode. The internal diameter of the low-voltage (LV) ground electrode was equal to the diameter of the HV electrode, and the external diameter of the LV electrode was 50 mm. To change the surface of the dielectric without changing the capacitance of the electrode system, PVC ($\varepsilon = 3$–$3.5$) $d = 0.3$ mm thick, or ceramics (MACOR, $d = 0.5$ mm, $\varepsilon = 5$–$6$), were glued to the grounded electrode by Geocel FIXER Mate silicon glue ($\varepsilon \approx 3$). The electrode system was installed in a constant volume chamber [7] allowing work at pressures 100 Torr $< P <$ 8 bar or in a high-pressure high-temperature chamber [8], 10 Torr $< P <$ 15 bar.

HV pulses, 20 ns in duration and 2 ns rise time, positive or negative polarity, 20–60 kV in amplitude on the HV electrode were delivered by the coaxial 30 m long 50 Ohm cable from the FPG20-03PM or FPG20-03PN pulser (FID Technology). A calibrated custom-made back current shunt installed in the center of the cable allowed measurements of current and voltage waveforms.

ICCD images ($\lambda = 300$–$800$ nm) were taken by a Pi-Max4 Princeton Instruments ICCD camera. Narrow-band optical filters (ThorLabs), FWHM = 10 nm were used for discharge ICCD imaging at a selected wavelength. Optical spectra, $\lambda = 250$–$500$ nm, were recorded by an ACTON spectrometer (SP-7500i, 600 I/mm grating) coupled with the ICCD camera.

Before the experiment, the discharge cell was pumped down to $10^{-2}$ Torr. $H_2$, $N_2$, $O_2$ and Ar (Air Liquide) with <100 ppm of impurities were used to prepare the mixtures. The experiments were carried out in a single shot regime at ambient initial temperature in air, $N_2$, $H_2$:$N_2$ = 1:4, $H_2$:$N_2$ = 1:59 and $O_2$:Ar = 2:3 mixtures.

## 3. Results

For any studied conditions, the emission intensity in filaments $I_f$ is tens of times higher than the emission between the filaments $I_f^0$ or in streamers $I_s$—the two last values are comparable. From figure 1 for synthetic air

$$I_f/I_f^0/I_s \approx 50/1.8/1. \quad (1)$$

Preliminary experiments revealed the two most important components in nitrogen-containing mixtures: bands of molecular nitrogen and the broadband continuum. To understand a spectral distribution of emission in space, a series of ICCD images with narrow band filters has been taken. The central wavelengths of the filter were selected to transmit 'only nitrogen emission' or 'only continuum emission'. Figure 2 presents typical images taken without and with the described filtering.

To distinguish the streamers from the filaments, we used the fact that in the few first nanoseconds, the nSDBD develops in a streamer mode. The discharge starts and develops during the first few nanoseconds with a typical velocity of a few mm/ns from the edge of the HV electrode. At this period, the optical emission from the discharge consists mainly of the bands of the second positive ($2^+$) system of molecular nitrogen. In the filamentary mode, two separate zones are clearly seen: the emission of the $2^+$ system corresponds to the zone 'around and ahead of' each filament, while the continuous wavelength (cw) emission comes from the filament core, or from the filament 'channel'. It should be noted that we do not analyze the discharge spectra in the direction perpendicular to the dielectric as a typical scale of changes in this direction is small compared to the resolution of the system.

Detailed spectral analysis demanded that we fix the position of the filament, so the discharge was stabilized in space using the technique suggested in [6] (the HV electrode has been replaced by a toothed wheel). A filament was selected and the discharge chamber rotated so that the filament was aligned with the spectrometer slit. The system provided temporal resolution of 0.5 ns and spatial resolution of 0.3 mm. To our knowledge, this is the first available data on time- and space-resolved emission of the filaments in nSDBD.

Figure 3 presents typical spectra of nSDBD as a function of wavelength and the distance from the HV electrode. The first three images (figures 3(a)–(c)) show spectra taken for positive polarity discharge. The inserts in the right upper corners provide the position of the ICCD gate relative to the voltage waveform. The emission of the $2^+$ band of $N_2$ is clearly seen

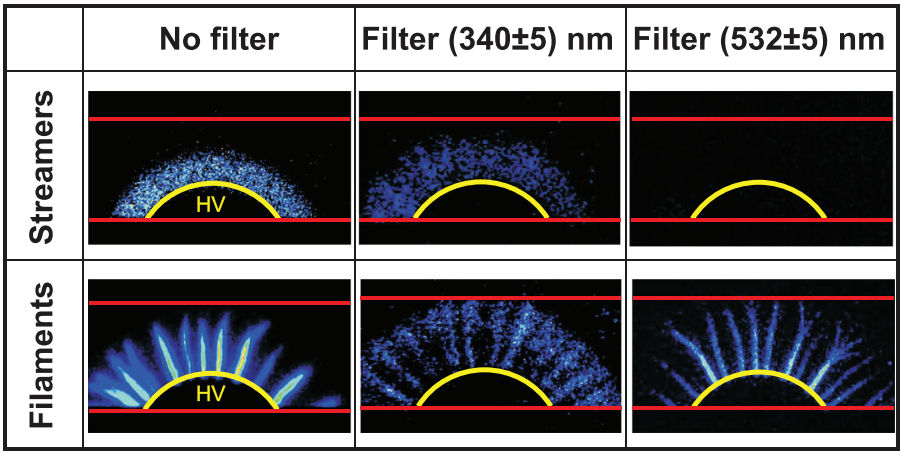


**Figure 2.** ICCD images of the streamer and filamentary mode with bandwidth filters. Streamers: time delay is 0 ns, camera gate is 5 ns; filaments: time delay is 5 ns, camera gate is 20 ns. Synthetic air, $U = -52$ kV, $P = 4$ bar.

in the propagating front (figure 3(a)). At $t \approx 2$ ns a streamer-to-filament transition occurs. The filaments propagate from the HV electrode as a wave of the cw emission. The start of the filaments corresponds to the regions 0–2 mm and 2–4 mm where the cw spectrum is already seen. The emission of the first negative system of $N_2^+$ at the regions 0–2 mm and 4–6 mm at 391.4 nm indicates high electric fields in the front of the discharge. When the filament is formed, the $N_2$ emission is replaced by cw emission, and the intensity of the $N_2$ emission drops dramatically (figure 3(b)). High voltage remains on the electrode, and the discharge propagates, leaving behind the front of a bright channel—a filament.

No well-defined atomic lines or molecular bands can be distinguished in the spectra for $\lambda = 250$–$500$ nm; a slight decrease of emission is observed after 400 nm. It should be noted that the absence of NO($\gamma$) emission, $NO(A^2\Sigma^+, v) \rightarrow NO(X^2\,\Pi, v') + h\nu$, at $\lambda < 300$ nm means an absence of high specific deposited energy. The electronically excited NO state is produced by electron impact and in the reaction $N_2(A^3\Sigma_u^+) + NO(X^2\Pi) \rightarrow N_2(X^1\Sigma_g^+, v) + NO(A^2\Sigma^+, v)$. At a low dissociation degree, the $NO(X^2\Pi)$ density is small [10], so no strong NO($\gamma$) emission is observed.

When the trailing edge of the pulse comes to the electrode, the second ionization wave starts and propagates on the trace of the filament. The second ionization wave contains the emission of the $2^+$ system of molecular nitrogen (see figure 3(c)) indicated on the electric field comparable to the fields in the discharge front. This emission was used to measure the rotational temperature on the trailing edge of the pulse.

An example of the emission of the negative polarity nSDBD is presented in figure 3(d). The intensity of the emission is systematically three to four times higher, and the shape is different compared to positive polarity discharge.

It should be noted that the integration of the emission over the distance from the HV electrode gives a picture similar to figure 1(c): the front of the signal is mainly due to $2^+$ emission of molecular nitrogen, and the 'body' of the emission profile, where the maximum of the emission is observed, is due to cw radiation.

The width of the selected spectral lines can answer the question regarding the electron density in the filaments. The experiments were carried out in 5 bar $H_2$:$N_2$ = 1:4 ($U > 0$), 6 bar $H_2$:$N_2$ = 1:59 ($U < 0$) and 5 bar $O_2$:Ar = 2:3 mixtures; lines of atomic hydrogen (656.3 nm, $H_\alpha$) and atomic oxygen (777.3 nm, $3^5P$–$3^5S$) have been analyzed. Continuous spectra similar to those measured in air were observed in both mixtures. Similar cw spectra in such different mixtures prove that the spectra are not due to a particular molecular continuum or molecular bands, like the continuum of molecular hydrogen or $NO_2^*$ emission [11]. The time instant of the appearance of the lines coincided with the appearance of the cw spectra.

Dynamics of the FWHM for $H_\alpha$ calculated from the Lorenz function is given by figure 4(a) for both polarities of the pulse, together with the waveforms of voltage on the HV electrode and electrical current for negative polarity discharge. The FWHM is enormously large in the discharge, 20–30 nm. Two decays are observed: the first one is in good correlation with the decay of the electrical current; the second is longer, already in the 'current-free' zone when the electron temperature is low. A typical time of 50% decrease of the FWHM is equal to 10–20 ns. Figure 4(b), presenting the FWHM for the 777 nm oxygen line, provides 15 ns decay, in correlation with $H_\alpha$. The FWHM itself is narrower for oxygen, 6 nm in the discharge, according to the idea that hydrogen is more sensitive to broadening. Figure 4(b) also shows cw emission in the vicinity of 777 nm, and the integral of the O-atom emission over the wavelength, proportional to $O(3^5P)$-atoms density. The FWHM of O-atoms practically does not change along the filament.

## 4. Discussion

No lines corresponding to the material of the electrode were detected in the spectra. No difference was found between the spectra for different dielectrics. PVC is produced by polymerization of $C_2H_3Cl$; ceramics consist of non-organic materials (for MACOR: $SiO_2$ (46%), $Al_2O_3$ (16%), MgO (17%), $KO_2$

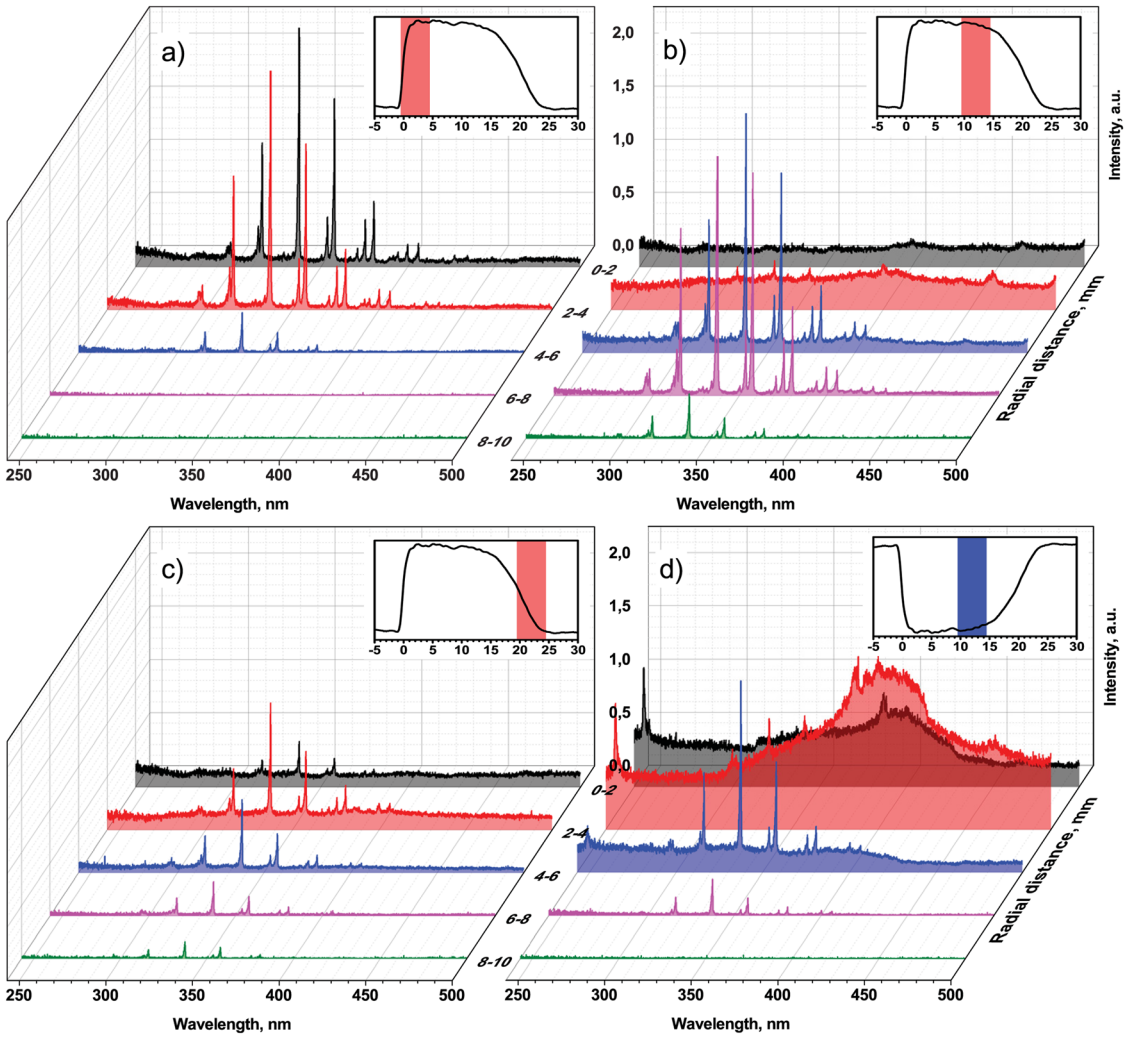


**Figure 3.** Time- and space-resolved spectra of (a)–(c) positive polarity and (d) negative polarity filamentary discharges. Synthetic air, $U = \pm 50$ kV, $P = 6$ bar. Inserts show the ICCD gate relative to the voltage waveform.

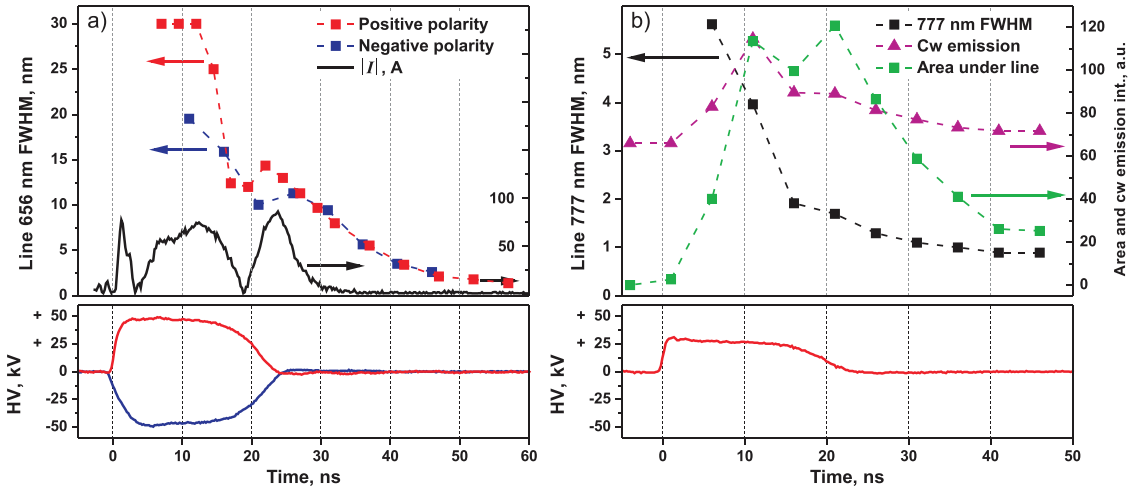


**Figure 4.** FWHMs versus time: (a) $H_\alpha$ superimposed with the voltage coming to the electrode and current through the discharge; (b) 777 nm of atomic oxygen superimposed with the voltage waveform, the area under the line and cw emission near 777 nm.

(10%), $B_2O_3$ (7%), F (4%)). Similar cw spectra prove that the emission does not originate from damaging the dielectric.

The spectrum is not a Planck emission. Indeed, the gas temperatures calculated from the rotational temperature at the rise front and trailing edge of the pulse do not differ significantly; in both instants, gas temperature is $T_g = 300$–$500$ K. The analysis of the radial distribution of the emission proves that the light comes from the central part of the channel, not from the surface. Finally, the most important evidence is a temporal behavior of the emission: if this was Planck radiation, it would increase with time corresponding to fast energy relaxation in the afterglow [12, 13]. This is not the case; the cw emission decreases within a few tens of nanoseconds, and hydrodynamic expansion on the time scale 50 ns is small to provide significant cooling. For the filament radius $r_f \approx 70$ $\mu$m [8] and $T_g = 500$ K, a gas-dynamic time is about 200 ns.

Continuum emission in visible and UV was recorded [14–17] in pulsed discharges in atmospheric pressure air. Atomic lines of materials of electrodes were observed [14]. More 'soft' spectra were obtained [16] in air at $P = 1$ atm and $U = 90$ kV; no materials of electrodes, but the lines of ionized nitrogen atoms were clearly seen. Similar spectra, with atomic N-ion lines dominating over the cw emission, were observed in the emission of constricted SDBD [17] powered by a burst of unipolar 400 $\mu$s pulses at $U = 20$ kV.

Nanosecond discharges excited in open atmosphere at high voltages, $U = 150$–$250$ kV, generate [14, 15] high energy runaway electrons and secondary x-ray bremsstrahlung. The nSDBD studied in the present work seems to be a discharge with significantly smaller specific deposited energy, and the question about the physics of the cw emission remains open. Experimental observations can be summarized in the following way: cw emission does not exist at the rising front of the pulse (figure 3(a)); the cw emission in the filaments and emission of the broad atomic lines appear at the same time and come from the same space region. Temporal behavior of the cw emission and of FWHM of the O-atom and H-atom lines is similar; typical decay comprises a few tens of nanoseconds (figure 4). The density of excited O-atoms estimated from the integral of emission at 777 nm has a similar shape but somewhat broader maximum, and is slightly delayed relative to the maximum of the FWHM.

Two types of emission due to high electron density can be considered here: bremsstrahlung and recombination radiation [18]. Bremsstrahlung originates from the acceleration of an electron in Coulomb collisions with ions. Energy per 1 $cm^3$ per second in an SGC system in assumption of the Maxwellian EEDF is written as

$$P_b = 1.5 \cdot 10^{-27} Z^2 n_e n_i \sqrt{T_e(\mathrm{K})}\,. \qquad (2)$$

Recombination radiation is the process of emitting the photon in recombination of the ion and electron, and can be expressed as

$$P_r = 5 \cdot 10^{-22} Z^4 n_e n_i \sqrt{1/T_e(\mathrm{K})}\,. \qquad (3)$$

Here $Z$ is a charge of ion, $n_e$, $n_i$ are electron and ion densities respectively, $T_e$ is electron temperature. The fact that $P_b = P_r$ at $T_e \approx 30$ eV means that in our case recombination radiation should dominate.

To get recombination radiation at the experimental conditions of nSDBD, the electron density in the filaments should be extremely high. If the broadening is due to electron density, a maximum value of $n_e^{max} \sim 10^{19}$ $cm^{-3}$ can be obtained from FWHM of $H_\alpha$ following the procedure described in [19].

High values of $n_e$ from $H_\alpha$ and N-atoms broadening were obtained earlier in $P = 1$ atm discharge in a $N_2$:$H_2O$ mixture for 9 kV/170 ns pulses [19]. Values up to $n_e = 4 \cdot 10^{18}$ $cm^{-3}$ ($n_e/N > 10\%$) with a long decay rate, $8.6 \cdot 10^6$ $s^{-1}$, are reported. The authors explain a long decay by additional production of electrons in the afterglow via Penning and associative ionization, and remark that the density of excited species should be comparable to $n_e$. At the same time, our estimates of energy release at such a high ionization degree give too high values of gas heating. In particular, in electron–ion recombination, $N_2^+ + e \rightarrow N(^4S,\ ^2D) + N(^2D)$, the energy $\Delta E = 2.25$ eV is released [20]; $\Delta E \approx 2$ eV is released in the quenching of $N(^2D)$ [21]. At $P = 760$ Torr and $T \geqslant 600$ K a characteristic quenching time of $N(^2D)$ does not exceed 130 ns [21]. About 90% of the difference between the ionization potential of molecular nitrogen, $I_{N_2} = 15.8$ eV and the dissociation energy, $D_{N_2} = 9.76$ eV at a typical time scale longer than 200–300 ns goes to the gas heating. At ionization degree $n_e/N \approx 10\%$, the estimates taking into account only the mentioned processes will result, after the hydrodynamic expansion, in a temperature increase $\Delta T_g = 1500$–$1600$ K, while the temperature increase measured in [19] at $t \geqslant 2$ $\mu$s is $\Delta T_g \leqslant 500$ K. However, as far as the temperature in [19] is measured by Rayleigh scattering with a given fixed beam width and location, the expected narrow filament size and the movement of the filament for different discharge events could lead to a measured gas temperature that is lower than the gas temperature in the core of the filament.

Although obtained in the present work extra-high $n_e$ values need additional verification, it is evident that the cw spectra correlate in time with high electron density. Filamentation triggers sharp increase of $n_e$. Highly conductive channels originated near the HV electrode were observed in [22], the propagation velocity of the channels (filaments) was $V = 5 \cdot 10^7$–$10^8$ cm $s^{-1}$. Contraction and the appearance of a bright channel has been observed before in high-power discharges [23, 24]. The formation of a current spot on the electrode is followed by the constriction of a stable homogeneous plasma column and the development of a bright channel propagating with $V = 10^4$–$10^6$ cm $s^{-1}$ [23]. High-current nanosecond discharge ($j \geqslant 100$ A $cm^{-2}$) constricted at moderate pressures, $P = 76$ Torr, produced high electron densities, $n_e \sim 10^{17}$ $cm^{-3}$, and propagated with $V \sim 10^6$–$10^7$ cm $s^{-1}$ [24].

In our case, the filamentation can be triggered by the formation of at least one current spot on the HV electrode. Both field emission and explosive emission can be important on this time scale [25]. Produced filament propagates from the electrode due to local enhancement of the electric field in the head, suppresses adjacent streamers because of high carried electric charge, and defines, by the value of the change, a

minimal possible distance between the filaments. Neighboring filaments follow the same rules, and in a few nanoseconds or less, a regular structure of filaments is formed around the HV electrode.

## 5. Conclusions

Streamer-to-filament transition is a characteristic feature of nSDBDs at high pressures and voltages. Bright optical emission from the filamentary nSDBD, 50 times more intense than the emission from the streamer nSDBD, is due to continuous wavelength radiation, intense in the UV and decreasing in the visible and IR regions. Space- and time-resolved emission from the surface filament has been measured for the first time. A continuum spectrum emits from the 'body' of the filament, mainly from the central part of the filament channel. The filaments are enveloped in a streamer-like emission (the second positive system of molecular nitrogen for nitrogen-containing mixtures).

It is suggested that the streamer-to-filament transition can be considered as the instability caused by current spots on the HV electrode. As a result, a regular structure of plasma channels with high electron density (filaments) is formed instead of streamers and propagates from the HV electrode as a second ionization wave. High electron densities are confirmed experimentally by space and time-resolved measurements of the FWHMs of the selected atomic lines. The distance between the filaments is regulated by the electrical charge of the individual filaments. The observed cw spectrum is presumably caused by the high density of the electrons.

## Acknowledgments

The work was partially supported by the French National Research Agency, ANR (PLASMAFLAME Project, 2011 BS09 025 01), AOARD AFOSR (FA2386-13-1-4064 grant), LabEx Plas@Par, RFBR (17-52-16001 grant) and Linked International Laboratory LIA KaPPA (France-Russia). The internship of A Yu Khomenko was supported by the Russian Ministry of Education and Science, program '5top100'.

## References

[1] Roupassov D V, Zavyalov I N, Starikovskii A Y and Saddoughi S G 2006 Boundary layer separation plasma control using low-temperature non-equilibrium plasma of gas discharge *44th AIAA Aerospace Sciences Meeting and Exhibit (Reno, Nevada, 9–12 January 2006)* AIAA 2006–373

[2] Leonov S B, Adamovich I V and Soloviev V R 2016 Dynamics of near-surface electric discharges and mechanisms of their interaction with the airflow *Plasma Sources Sci. Technol.* **25** 063001

[3] Treschalov A B and Lisovskiy A A 2012 Source of the VUV radiation on the basis of surface discharge *Opt. J.* **79** 15–23 (in Russian)

[4] Allegraud K, Guaitella O, Kosarev I N, Mintusov E I, Pendleton S J, Popov N A, Sagulenko P N, Rousseau A and Starikovskaia S M 2010 Surface discharges: possible applications for plasma-assisted ignition and electric field measurements *Proc. 48th AIAA Aerospace Sciences Meeting including the New Horizons Forum and Aerospace Exposition (Orlando, FL, USA, January 2010)* AIAA-2010-1587

[5] Kosarev I N, Khorunzhenko V I, Mintoussov E I, Sagulenko P N, Popov N A and Starikovskaia S M 2012 A nanosecond surface dielectric barrier discharge at elevated pressures: time-resolved electric field and efficiency of initiation of combustion *Plasma Sources Sci. Technol.* **21** 045012

[6] Anokhin E M, Kuzmenko D N, Kindysheva S V, Soloviev V R and Aleksandrov N L 2015 Ignition of hydrocarbon: air mixtures by a nanosecond surface dielectric barrier discharge *Plasma Sources Sci. Technol.* **24** 045014

[7] Stepanyan S A, Starikovskiy A Y, Popov N A and Starikovskaia S M 2014 A nanosecond surface dielectric barrier discharge in air at high pressures and different polarities of applied pulses: transition to filamentary mode *Plasma Sources Sci. Technol.* **23** 045003

[8] Shcherbanev S A, Popov N A and Starikovskaia S M 2017 Ignition of high pressure lean $H_2$: air mixture along the multiple channels of nanosecond surface discharge *Combust. Flame* **176** 272–84

[9] Boumehdi M A, Stepanyan S A, Desgroux P, Vanhove G and Starikovskaia S M 2015 Ignition of methane- and n-butane-containing mixtures at high pressures by pulsed nanosecond discharge *Combust. Flame* **162** 1336–49

[10] Popov N A 2016 Pulsed nanosecond discharge in air at high specific deposited energy: fast gas heating and active particles production *Plasma Sources Sci. Technol.* **25** 044003

[11] Okabe H 1978 *Photochemistry of Small Molecules* (New York: Wiley)

[12] Rusterholtz D L, Lacoste D A, Stancu G D, Pai D Z and Laux C O 2013 Ultrafast heating and oxygen dissociation in atmospheric pressure air by nanosecond repetitively pulsed discharges *J. Phys. D: Appl. Phys.* **46** 464010 (21pp)

[13] Klochko A V, Lemainque J, Booth J-P and Starikovskaia S M 2015 TALIF measurements of oxygen atom density in the afterglow of a capillary nanosecond discharge *Plasma Sources Sci. Technol.* **24** 025010

[14] Babich L P, Loiko T V and Tsukerman V A 1990 High-voltage nanosecond discharge in a dense gas at a high overvoltage with runaway electrons *Sov. Phys.—Usp.* **33** 521–40

[15] Babich L P and Loiko T V 2010 Peculiarities of detecting pulses of runaway electrons and x-rays generated by high-voltage nanosecond discharges in open atmosphere *Plasma Phys. Rep.* **36** 263–270

[16] Shao T, Tarasenko V F, Zhang Ch, Lomaev M I, Sorokin D A, Yan P, Kozyrev A V and Baksht E Kh 2012 Spark discharge formation in an inhomogeneous electric field under conditions of runaway electron generation *J. Appl. Phys.* **111** 023304

[17] Houpt A W and Leonov S B 2016 Charge transfer in constricted form of surface barrier discharge at atmospheric pressure *J. Thermophys. Heat Transfer* at press (doi: 10.2514/1.T4970)

[18] Artsimovich L A and Sagdeev R Z 1979 *Physics of Plasmas for Physicists* (Moscow: Atomizdat)

[19] Van der Horst R M, Verreycken T, Van Veldhuizen E M and Bruggeman P J 2012 Time-resolved optical emission spectroscopy of nanosecond pulsed discharges in atmospheric-pressure $N_2$ and $N_2/H_2O$ mixtures *J. Phys. D: Appl. Phys.* **45** 345201

[20] Mintoussov E I, Pendleton S J, Gerbault F G, Popov N A and Starikovskaia S M 2011 Fast gas heating in nitrogen–oxygen discharge plasma: II. Energy exchange in the afterglow of a volume nanosecond discharge at moderate pressures *J. Phys. D: Appl. Phys.* **44** 285202

[21] Galvao B R L, Braga J P, Belchior J C and Varandas A J C 2014 Electronic quenching in $N(^2D) + N_2$ collisions: a state-specific analysis via surface hopping dynamics *J. Chem. Theory Comput.* **10** 1872–7

[22] Shcherbanev S A, Stepanyan S A, Popov N A and Starikovskaia S M 2015 Dielectric barrier discharge for multi-point plasma-assisted ignition at high pressures *Phil. Trans. R. Soc.* A **373** 20140342

[23] Akishev Yu, Karalnik V, Kochetov I, Napartovich A and Trushkin N 2014 High-current cathode and anode spots in gas discharges at moderate and elevated pressures *Plasma Sources Sci. Technol.* **23** 054013

[24] Genkin S A, Kozurev A V, Korolev Yu D and Tipchurin K A 1985 *Zurnal Techn. Phys.* **55** 1216 (in Russian)

[25] Levko D, Yatom S, Vekselman V and Krasik Ya E 2012 Electron emission mechanism during the nanosecond high-voltage pulsed discharge in pressurized air *Appl. Phys. Lett.* **100** 084105